

Co-ordination Chemistry of Mixed Pyridine–Phenol Ligands: Polynuclear Complexes of 6-(2-Hydroxyphenyl)-2,2'-bipyridine with Ni^{II}, Cd^{II}, Mn^{II} and Mn^{II}Mn^{III}[†]

David A. Bardwell, John C. Jeffery and Michael D. Ward *

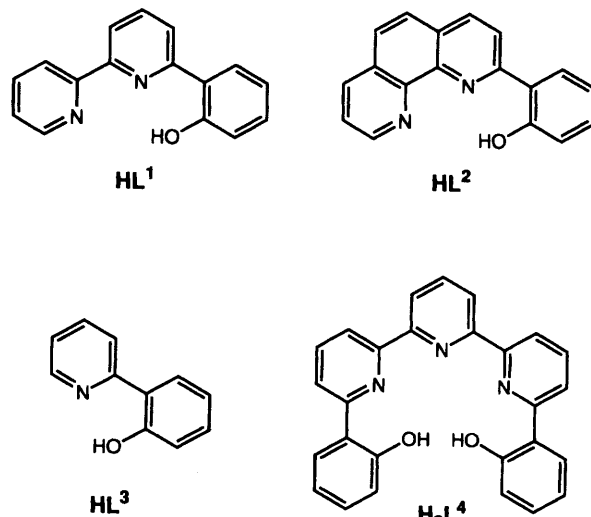
School of Chemistry, University of Bristol, Cantock's Close, Bristol BS8 1TS, UK

A series of complexes with the N,N,O-terdentate ligand 6-(2-hydroxyphenyl)-2,2'-bipyridine (HL^1) has been prepared and structurally characterised. The complexes are $[\text{Ni}_2\text{L}^1_2(\text{dmf})_2(\text{H}_2\text{O})_2][\text{BPh}_4]_2$ **1**, $[\text{Cd}_2\text{L}^1_2(\text{HL}^1)(\text{dmf})_2][\text{BPh}_4]_2$ **2**, $[\text{Mn}_4\text{L}^1_6][\text{BPh}_4]_2$ **3** and $[\text{Mn}_2\text{L}^1_3(\text{MeCN})][\text{PF}_6]_2$ **4**. In the centrosymmetric complex **1** one ligand L^1 is associated with each metal but the phenolates are bridging, giving a $\text{Ni}^{II}(\mu\text{-O})_2$ core; the remaining two co-ordination sites are occupied by H_2O and dmf (O-co-ordinated) ligands. In complex **2** one Cd^{II} ion is octahedrally co-ordinated by two ligands L^1 ; the two phenolates bridge to the second Cd^{II} , whose co-ordination sphere is completed by two dmf ligands and the two pyridyl donors of another equivalent of HL^1 , whose pendant phenol remains protonated and forms hydrogen-bonding interactions to lattice solvent molecules. Complex **3** in contrast is an unusual example of a linear chain, with a $\text{Mn}^{II}(\mu\text{-O})_2\text{Mn}^{II}(\mu\text{-O})_2\text{Mn}^{II}(\mu\text{-O})_2\text{Mn}^{II}$ core (where O denotes a bridging phenolate) and highly distorted six-co-ordinate Mn^{II} centres: the chain formation is apparently facilitated by the absence of any stereoelectronic preference for the Mn^{II} ions which can readily tolerate the distorted geometries. Complex **4** contains a Mn^{II} centre, co-ordinated by two ligands L^1 , and a Mn^{III} centre which shares two phenolates with the Mn^{II} and also has a terdentate L^1 and a MeCN ligand to complete the co-ordination sphere. The Mn^{III} centre shows Jahn-Teller elongation along one of the axes. The contributions of factors such as the metal oxidation state, the co-ordination modes available to the ligand, and non-covalent interactions (hydrogen bonding, aromatic π -stacking) to the structures of the complexes are discussed.

We have recently been studying the structures and properties of transition-metal complexes of polydentate ligands such as HL^1 – HL^4 which contain mixed pyridine and phenolate donor sets.^{1–4} Bridging of the phenolate donors to two metal ions can result in the formation of binuclear^{2,3} and tetranuclear⁴ species which show magnetic exchange interactions between the metal centres. It has become apparent that unless the metal ion has a particularly strong stereoelectronic preference (e.g. Co^{3+} , Pd^{2+}) the structures of the complexes are highly unpredictable and do not show any simple systematic features which can be related to the known properties of the metal or ligand component parts. Rawson and Winpenny⁵ have likewise shown that simple potentially bridging ligands such as 2-hydroxypyridine derivatives can form complexes with first-row transition metals whose structural complexity is in some cases out of all proportion to the simplicity of the component parts. We have been interested in a systematic study of the structures of complexes with these simple ligands with various transition-metal ions, and we describe here the preparation and crystal structures of complexes of L^1 with Ni^{II} , Mn^{II} and Mn^{III} , and Cd^{II} , all of which are at least binuclear by virtue of phenolate bridges between adjacent pairs of metal centres. The complexes are $[\text{Ni}_2\text{L}^1_2(\text{dmf})_2(\text{H}_2\text{O})_2][\text{BPh}_4]_2$ **1**, $[\text{Cd}_2\text{L}^1_2(\text{HL}^1)(\text{dmf})_2][\text{BPh}_4]_2$ **2**, $[\text{Mn}_4\text{L}^1_6][\text{BPh}_4]_2$ **3** and $[\text{Mn}_2\text{L}^1_3(\text{MeCN})][\text{PF}_6]_2$ **4**.

Experimental

Instrumentation used for routine spectroscopic methods has been described previously.^{1–4} Ligand HL^1 was prepared as



described earlier.⁶ Metal salts and organic starting materials were purchased from Aldrich and used as received.

Preparations.—All of the complexes were prepared in the same way. Equimolar amounts of the appropriate metal acetate hydrate and HL^1 were stirred in MeOH for 1 h. For **1**–**4** the metal salts used were $\text{Ni}(\text{MeCO}_2)_2 \cdot 4\text{H}_2\text{O}$, $\text{Cd}(\text{MeCO}_2)_2 \cdot 2\text{H}_2\text{O}$, $\text{Mn}(\text{MeCO}_2)_2 \cdot 4\text{H}_2\text{O}$ and $\text{Mn}(\text{MeCO}_2)_3 \cdot 2\text{H}_2\text{O}$ respectively. Dropwise addition of an aqueous solution of NaBPh_4 (for **1**–**3**) or KPF_6 (for **4**) followed by cooling resulted in precipitation of the complexes which were collected by filtration and dried before recrystallisation as described below. Elemental analyses of the recrystallised materials are given in Table 1.

[†] Supplementary data available: see Instructions for Authors, *J. Chem. Soc., Dalton Trans.*, 1995, Issue 1, pp. xxv–xxx.

Table 1 Elemental analytical data for the new complexes

Complex	Analytical data * (%)		
	C	H	N
1·4dmf	68.0 (68.3)	6.4 (6.3)	7.7 (8.1)
2·2dmf	68.3 (68.3)	5.5 (5.4)	7.2 (7.4)
3·MeCN	73.4 (73.6)	4.6 (4.6)	7.7 (7.6)
4	50.3 (50.8)	2.8 (3.0)	8.0 (8.3)

* Calculated values in parentheses. The analytical data for **1–3** are consistent with retention of some or all of the solvent of crystallisation.

Crystal-structure Determinations.—Crystals were grown from the following solvents: **1**, dimethylformamide (dmf)–Et₂O (pale green blocks); **2**, dmf–Et₂O (colourless blocks); **3**, MeCN–Et₂O (orange needles); **4**, MeCN–Et₂O (dark brown blocks). In all cases the second named solvent was carefully layered onto a concentrated solution of the complex in the first solvent. Crystals usually appeared in a few days at the interface; if not, the mixture was refrigerated at –20 °C for several days. The crystals selected were sealed in glass capillary tubes with some of the mother liquor present, as a precaution against solvent loss. Data were collected using a Siemens R3m/V four-circle diffractometer (293 K, Mo-K α X-radiation, graphite monochromator, $\lambda = 0.710\,73 \text{ \AA}$, Wyckoff ω scans). The data were corrected for Lorentz and polarisation effects, and for absorption effects using an empirical method based on azimuthal scan data.⁷ Details of the crystal data, intensity collection and refinements are summarised in Table 2.

All structures were solved by conventional heavy-atom or direct methods using SHELXTL PLUS on a DEC micro-Vax II computer; the least-squares refinements (on all F^2 data) were then carried out on a Silicon Graphics Indigo R4000 computer using SHELX 93.⁷ Successive Fourier-difference syntheses were used to locate all non-hydrogen atoms; hydrogen atoms were included in calculated positions. Scattering factors with corrections for anomalous dispersion were taken from ref. 8. Selected bond lengths and angles for **1–4** are in Tables 3, 5, 7 and 9 respectively; atomic coordinates are in Tables 4, 6, 8 and 10.

Additional material available from the Cambridge Crystallographic Data Centre comprises H-atom coordinates, thermal parameters and remaining bond lengths and angles.

Results and Discussion

Complex 1.—Reaction of Ni(MeCO₂)₂·4H₂O with 1 equivalent of HL¹ in methanol afforded a pale green solution from which a precipitate was isolated on addition of NaBPh₄. A FAB mass spectrum of this material gave peaks at *m/z* 305, 553 and 610 corresponding to {NiL¹}, {NiL¹₂} and {Ni₂L¹₂} fragments, indicating that a binuclear complex had formed. Recrystallisation from dmf–diethyl ether afforded pale green blocks of 1·4dmf whose X-ray structure (Fig. 1; Tables 3 and 4) reveals a binuclear, centrosymmetric structure. Each ligand L¹ donates its two pyridyl ligands to one metal and then shares the phenolate between both metals, resulting in a Ni₂(μ-O)₂ core. The remaining two co-ordination sites on each centre are occupied by one water molecule and one O-bound dmf molecule. The co-ordination geometry about each Ni^{II} is approximately octahedral with bond lengths in the range 1.99–2.12 Å. The bonds in the Ni₂(μ-O)₂ bridge display a short/long alternation [Ni–O(30) 2.121(4), Ni–O(30a) 1.993(4) Å]. The centre of symmetry requires that whereas one ligand L¹ is ‘above’ the Ni₂(μ-O)₂ plane the other is ‘below’ it, *i.e.* there is no π stacking arising from overlap of aromatic rings in the ligands. Such stacking interactions between ligands have been frequently observed in complexes with ligands of this type^{4,6,9} and presumably provide an additional stabilising influence,

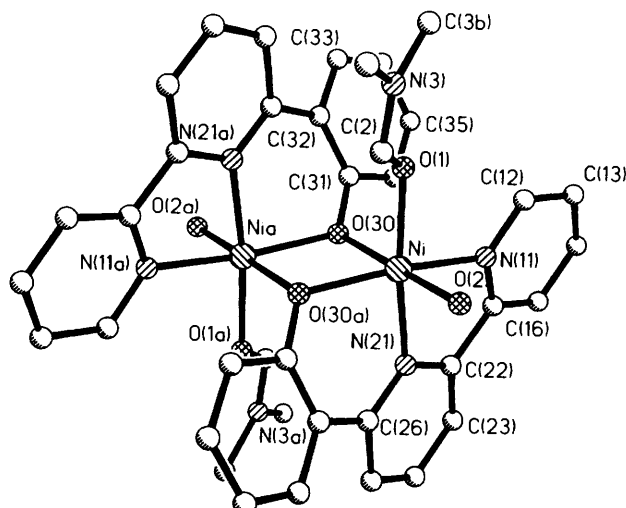


Fig. 1 Crystal structure of the cation of **1**

although they are clearly not essential in this case. There are many similarities between this structure and that of [Ni₂L³₂(dmf)₆][BPh₄]₂.³ The two hydrogen atoms of the co-ordinated water molecule on each Ni^{II} centre form hydrogen bonds to the oxygen atoms of dmf molecules in the lattice [H(water) ··· O(dmf) 2.033 and 2.004 Å].

There are many examples of dmf complexes with first-row transition metals,^{10,11} although few have been crystallographically characterised. The Ni–O(dmf) bond length [2.053(4) Å] is typical of those of other first-row M^{II} complexes;^{10,12} the low C=O stretching frequency of the co-ordinated dmf ligand of **1** (1654 cm⁻¹, KBr disc; *cf.* 1680 cm⁻¹ for free dmf) is usual for O-co-ordinated amide ligands and is a consequence of the π-acceptor nature of the carbonyl group.^{11,13}

One of the most significant features of this structure is the fact that it is completely different from that of [{NiL¹–(HL¹)₂}][PF₆]₂, in which two mononuclear, octahedral [NiL¹(HL¹)]⁺ fragments are held together by strong O–H ··· O hydrogen bonds between the (protonated) phenol and (deprotonated) phenolate ligands of adjacent Ni^{II} units: the phenolate ligands do not act as bridges.⁹ This observation underlines the unpredictable nature of complexes formed by these ligands—the same metal starting material [nickel(II) acetate] reacted with the same ligand under the same conditions can give different products depending on the counter-ion and the recrystallisation solvent. In the case of **1** the role of the recrystallisation solvent in controlling the structure is obvious since there are co-ordinated dmf ligands, and lattice dmf molecules stabilise the co-ordinated water ligands by hydrogen bonding. Unfortunately we were unable to obtain good crystals from any other solvent combination. We suspect that the initially formed complex (in the presence of water) is [Ni₂L¹₂(H₂O)₄]²⁺, and that during recrystallisation labile water ligands are in exchange with dmf solvent molecules: the form that is isolated is just the one which crystallises most readily. Formation of **1** is not solely controlled by a 1:1 metal:ligand ratio in the reaction since **1** was obtained even in the presence of excess HL¹.

The crystal structures of complex **1** and all previously reported complexes with L¹ involve metal cations with a definite stereoelectronic preference (Cu^{II}, Ni^{II}, Co^{III}, Pd^{II}, *etc.*). Although the resulting complexes display a variety of stoichiometries and structures they are all partially controlled by the stereoelectronic preference of the metal: thus **1** and [{NiL¹(HL¹)₂}][PF₆]₂, although very different, both have a requirement for octahedral geometry at the metal centres, which must limit to some extent the behaviour shown by the ligand. Accordingly we decided to investigate next the

Table 2 Summary of crystal details, data collection and refinement for complexes 1–4

Complex	1·4dmf	2·2dmf	3·2MeCN·2·5Et ₂ O	4·Et ₂ O
Formula	C ₉ H ₁₀ B ₂ N ₁₀ Ni ₂ O ₁₀	C ₁₀ H ₁₀ B ₂ Cd ₂ N ₁₀ O ₇	C ₁₅ H ₁₃ ⁷ B ₂ Mn ₂ N ₁₄ O _{8·5}	C ₅ H ₆ F ₁₂ Mn ₂ N ₇ O ₄ P ₂
<i>M</i>	1724.98	1898.42	2609.20	1256.80
Crystal system	Monoclinic	Monoclinic	Triclinic	Monoclinic
Space group	<i>P</i> 2 ₁ / <i>c</i>	<i>P</i> 2 ₁ / <i>c</i>	<i>P</i> 1	<i>P</i> 2 ₁ / <i>c</i>
<i>a</i> /Å	11.297(6)	32.88(2)	14.789(7)	11.568(7)
<i>b</i> /Å	23.92(2)	10.903(4)	17.730(10)	16.674(8)
<i>c</i> /Å	17.270(9)	29.23(2)	29.79(2)	28.526(11)
α°	90	90	84.42(4)	90
β°	96.47(4)	114.45(4)	82.62(4)	100.33(4)
γ°	90	90	68.47(4)	90
<i>U</i> /Å ³	4636(5)	9541(8)	7196(6)	5413(5)
<i>Z</i>	2	4	2	4
<i>D</i> _e /g cm ⁻³	1.236	1.322	1.204	1.542
$\mu/(Mo-K\alpha)/mm^{-1}$	0.269	0.507	0.404	0.620
<i>F</i> (000)	1824	3928	2722	2556
Crystal dimensions/mm	0.7 × 0.4 × 0.2	0.6 × 0.4 × 0.4	0.8 × 0.4 × 0.3	0.8 × 0.7 × 0.7
Unique reflections measured	4323	12461	13415	9522
2θ range/ ^o	4–40	5–45	4–40	4–50
Index ranges	0 ≤ <i>h</i> ≤ 10, 0 ≤ <i>k</i> ≤ 23, -16 ≤ <i>l</i> ≤ 16	-35 ≤ <i>h</i> ≤ 32, -11 ≤ <i>k</i> ≤ 0, 0 ≤ <i>l</i> ≤ 31	0 ≤ <i>h</i> ≤ 14, -15 ≤ <i>k</i> ≤ 17, -28 ≤ <i>l</i> ≤ 28	0 ≤ <i>h</i> ≤ 11, 0 ≤ <i>k</i> ≤ 19, -33 ≤ <i>l</i> ≤ 33
Data, restraints, parameters	4323, 38, 551	12457, 8, 1133	13408, 114, 1650	9518, 7, 731
Final residuals <i>wR</i> ₂ , <i>R</i> ₁	0.173, 0.062	0.137, 0.056	0.293, 0.083	0.245, 0.078
Weighting factors <i>a</i> , <i>b</i> *	0.0862, 6.4889	0.0418, 12.0827	0.1627, 8.0472	0.1195, 13.88
Largest difference peak, hole/e Å ⁻³	0.514, -0.363	0.774, -0.772	0.934, -0.354	1.019, -0.590

* Structure was refined on *F*_o² using all data: *wR*₂ = {Σ[w(*F*_o² - *F*_c²)²]Σw(*F*_o²)}/[Σw(*F*_o²) + (*aP*)² + *bP*] and *P* = [max(*F*_o², 0) + 2*F*_c²]/3. The value *R*₁ is given for comparison with older refinements based on *F*_o with a typical threshold of *F* ≥ 4σ(*F*) and *R*₁ = Σ|*F*_o| - |*F*_c|/Σ|*F*_o| and *w*₁ = [*σ*²(*F*_o) + *gF*_o²].

co-ordination behaviour of L^1 to metal ions with no stereoelectronic preference for any geometry, *i.e.* with d^{10} or high-spin d^5 configurations, to see how the ligands behaved in the absence of metal-directed control of geometry.

Complex 2.—Reaction of $Cd(MeCO_2)_2 \cdot 2H_2O$ with HL^1 followed by treatment with $NaBPh_4$ afforded a cream-coloured solid whose FAB mass spectrum showed peaks at m/z 969, 609 and 361 (based on ^{114}Cd) which correspond to the species $\{Cd_2L^1_3\}$, $\{CdL^1(HL^1)\}$ and $\{CdL^1\}$, again suggesting formation of a binuclear complex. The crystal structure of the material obtained after recrystallisation from dmf-diethyl ether (Fig. 2, Tables 5 and 6) confirmed formation of the binuclear complex $[Cd_2L^1_2(HL^1)(dmf)]_2[BPh_4]_2 \cdot 2dmf$ (**2**-2dmf). One metal atom [$Cd(1)$] is in an irregular six-co-ordinate *cis*- N_4O_2 environment provided by two meridionally-bound L^1 ligands. The two phenolates bridge to $Cd(2)$, which also has two O-bound dmf ligands and a molecule of HL^1 co-ordinated *via* the two pyridyl donors with the phenol group pendant, and is therefore in an irregular *cis*- N_2O_4 environment. The Cd -O bond lengths in the bridge are comparable to those of other phenolate-bridged binuclear cadmium(II) complexes.¹⁴ The

arrangement of ligands L^1 is such that the co-ordinated bipyridyl fragment of HL^1 on $Cd(2)$ lies stacked with two of the aromatic rings of one of the L^1 ligands on $Cd(1)$. The pendant, protonated phenol of HL^1 on $Cd(2)$ is stabilised by hydrogen bonding to the oxygen atoms of one of the lattice dmf molecules [$H(\text{phenol}) \cdots O(\text{dmf})$ 1.972 Å]. It would normally be expected that the entropic stabilisation provided by the chelate effect would favour co-ordination of this (deprotonated) phenol at one of the sites occupied by dmf, but the stabilisation provided by hydrogen bonding appears to overcome this, a form of behaviour we have observed in other polydentate ligands containing phenol residues.² The arguments that apply to complex **1**, concerning the possibility of a complex equilibrium of several species in solution from which one stable crystalline form precipitates, also apply to **2**. The co-ordinated

Table 3 Selected bond lengths (Å) and angles (°) for **1**

Ni–O(1)	2.053(4)	Ni–O(2)	2.112(4)
Ni–O(30)	2.121(4)	Ni–O(30a)	1.993(4)
Ni–N(11)	2.035(5)	Ni–N(21)	2.019(5)
C(2)–O(1)	1.224(7)		
O(30a)–Ni–N(21)	90.3(2)	O(30a)–Ni–O(1)	166.2(2)
N(21)–Ni–N(11)	80.2(2)	O(30a)–Ni–O(1)	96.4(2)
N(21)–Ni–O(1)	172.8(2)	N(11)–Ni–O(1)	93.6(2)
O(30a)–Ni–O(2)	96.1(2)	N(21)–Ni–O(2)	90.7(2)
N(11)–Ni–O(2)	94.0(2)	O(1)–Ni–O(2)	86.1(2)
O(30a)–Ni–O(30)	80.8(2)	N(21)–Ni–O(30)	92.5(2)
N(11)–Ni–O(30)	89.6(2)	O(1)–Ni–O(30)	91.0(2)
O(2)–Ni–O(30)	175.6(2)		

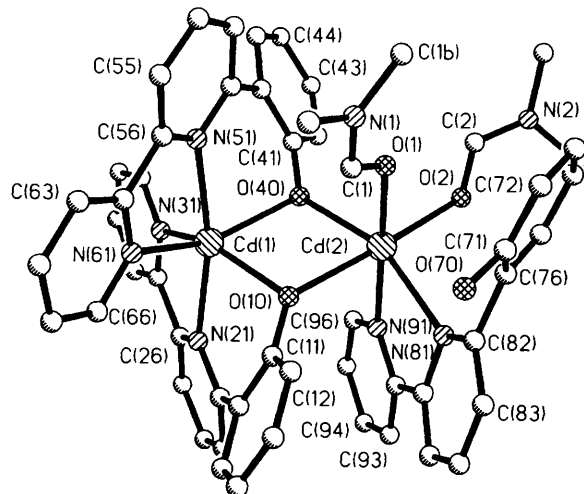


Fig. 2 Crystal structure of the cation of **2**

Table 4 Atomic coordinates ($\times 10^4$) for **1** with estimated standard deviations (e.s.d.s) in parentheses

Atom	<i>x</i>	<i>y</i>	<i>z</i>	Atom	<i>x</i>	<i>y</i>	<i>z</i>
Ni	1135(1)	5063(1)	5605(1)	C(105)	5240(9)	1900(5)	4601(6)
O(1)	1906(4)	4331(2)	5295(3)	C(106)	4297(8)	1887(4)	5073(5)
C(2)	2507(7)	4314(3)	4749(4)	C(111)	2332(6)	782(3)	6057(4)
N(3)	3128(6)	3882(3)	4570(4)	C(112)	1772(8)	355(4)	5608(5)
C(3a)	3865(10)	3910(5)	3924(6)	C(113)	1687(9)	-191(4)	5852(6)
C(3b)	3126(9)	3367(3)	5021(6)	C(114)	2150(8)	-337(4)	6586(7)
O(2)	2856(4)	5414(2)	5648(3)	C(115)	2677(9)	67(4)	7066(5)
N(11)	1309(5)	4869(2)	6759(3)	C(116)	2756(7)	611(3)	6805(5)
C(12)	1781(7)	4403(3)	7087(4)	C(121)	1308(6)	1564(3)	5107(4)
C(13)	1714(8)	4275(4)	7859(5)	C(122)	1310(7)	1762(3)	4353(4)
C(14)	1098(9)	4623(5)	8286(5)	C(123)	282(9)	1876(3)	3870(4)
C(15)	580(8)	5102(4)	7958(4)	C(124)	-813(8)	1813(3)	4115(5)
C(16)	718(6)	5217(3)	7184(4)	C(125)	-870(7)	1629(3)	4871(5)
N(21)	507(4)	5775(2)	6037(3)	C(126)	158(8)	1506(3)	5339(4)
C(22)	264(6)	5726(3)	6786(4)	C(131)	2747(6)	1884(3)	6388(4)
C(23)	-335(7)	6151(4)	7127(5)	C(132)	3777(7)	1884(3)	6912(5)
C(24)	-653(8)	6627(4)	6718(6)	C(133)	3992(8)	2272(4)	7516(5)
C(25)	-354(7)	6685(3)	5975(5)	C(134)	3187(9)	2690(4)	7602(5)
C(26)	238(6)	6249(3)	5625(4)	C(135)	2171(8)	2719(3)	7089(5)
O(30)	-575(4)	4686(2)	5475(2)	C(136)	1959(7)	2321(3)	6501(4)
C(31)	-705(6)	4151(3)	5676(4)	C(201)	5190(15)	5772(10)	3192(13)
C(32)	-582(6)	3695(3)	5171(4)	C(202)	4147(13)	6776(7)	3328(12)
C(33)	-744(6)	3159(3)	5460(5)	N(203)	4428(9)	6187(5)	3540(8)
C(34)	-990(7)	3062(3)	6208(5)	C(204)	3857(13)	6101(8)	4200(9)
C(35)	-1083(6)	3507(4)	6700(4)	O(205)	4034(9)	5553(5)	4365(5)
C(36)	-963(6)	4041(3)	6440(4)	C(300)	3485(28)	5720(14)	8793(12)
B(100)	2500(7)	1413(3)	5692(4)	C(301)	2918(22)	6462(11)	8173(20)
C(101)	3667(7)	1402(3)	5188(4)	N(302)	3432(15)	5911(9)	7972(10)
C(102)	4037(8)	934(4)	4815(5)	C(303)	3603(19)	5836(7)	7185(12)
C(103)	4968(12)	946(6)	4351(7)	O(304)	3244(19)	6300(8)	6825(10)
C(104)	5549(10)	1433(7)	4253(6)				

dmf molecules give strong bands in the IR spectrum at 1654 and 1639 cm⁻¹. We cannot tell whether the latter two peaks arise from dmf ligands in different environments, or from a degree of coupling to give symmetric and asymmetric vibrations.

Complex 3.—Reaction of Mn(MeCO₂)₂·4H₂O with HL¹ in methanol followed by addition of NaBPh₄ afforded a yellow-orange solid. A FAB mass spectrum showed peaks at *m/z* 302, 550 and 851, corresponding to the fragments {MnL¹}, {MnL₂} and {Mn₂L₃}, indicating that at least a binuclear

Table 5 Selected bond lengths (Å) and angles (°) for **2** with e.s.d.s in parentheses

Cd(1)-O(10)	2.226(4)	Cd(2)-O(40)	2.238(4)
Cd(1)-O(40)	2.249(5)	Cd(2)-O(1)	2.250(5)
Cd(1)-N(31)	2.284(6)	Cd(2)-O(2)	2.283(5)
Cd(1)-N(61)	2.287(6)	Cd(2)-O(10)	2.310(4)
Cd(1)-N(51)	2.341(5)	Cd(2)-N(91)	2.320(6)
Cd(1)-N(21)	2.346(5)	Cd(2)-N(81)	2.347(6)
O(10)-Cd(1)-O(40)	77.8(2)	O(40)-Cd(2)-O(1)	88.8(2)
O(10)-Cd(1)-N(31)	145.9(2)	O(40)-Cd(2)-O(2)	97.6(2)
O(40)-Cd(1)-N(31)	92.9(2)	O(1)-Cd(2)-O(2)	90.2(2)
O(10)-Cd(1)-N(61)	92.1(2)	O(40)-Cd(2)-O(10)	76.3(2)
O(40)-Cd(1)-N(61)	146.1(2)	O(1)-Cd(2)-O(10)	93.4(2)
N(31)-Cd(1)-N(61)	111.7(2)	O(2)-Cd(2)-O(10)	172.9(2)
O(10)-Cd(1)-N(51)	107.3(2)	O(40)-Cd(2)-N(91)	93.2(2)
O(40)-Cd(1)-N(51)	80.2(2)	O(1)-Cd(2)-N(91)	175.8(2)
N(31)-Cd(1)-N(51)	103.2(2)	O(2)-Cd(2)-N(91)	93.2(2)
N(61)-Cd(1)-N(51)	71.9(2)	O(10)-Cd(2)-N(91)	83.5(2)
O(10)-Cd(1)-N(21)	80.9(2)	O(40)-Cd(2)-N(81)	157.9(2)
O(40)-Cd(1)-N(21)	110.3(2)	O(1)-Cd(2)-N(81)	105.7(2)
N(31)-Cd(1)-N(21)	71.6(2)	O(2)-Cd(2)-N(81)	98.9(2)
N(61)-Cd(1)-N(21)	99.7(2)	O(10)-Cd(2)-N(81)	86.0(2)
N(51)-Cd(1)-N(21)	168.2(2)	N(91)-Cd(2)-N(81)	71.4(2)

complex had formed. Crystals were grown from acetonitrile-diethyl ether and the X-ray structure (Fig. 3, Tables 7 and 8) shows the complex to be [Mn₄L¹₆][BPh₄]₂·2MeCN·2.5Et₂O (3·2MeCN·2.5Et₂O), in which the complex cation has a structure very similar to that of [Mn₄L²₆][ClO₄]₂.⁴ The complex cation contains a chain of four crystallographically independent Mn^{II} ions, all of which are six-co-ordinate. The two terminal Mn^{II} ions each have *cis*-N₄O₂ donor sets from two terdentate L¹ ligands, with the two phenolates bridging to the inner Mn^{II} ions. The two inner Mn^{II} ions each have one associated terdentate ligand, with the other three sites occupied by bridging phenolates from ligands on neighbouring metals, and therefore have *cis*-N₂O₄ donor sets. The result is a Mn(μ -O)₂Mn(μ -O)₂Mn(μ -O)₂Mn chain (where O denotes a phenolate ligand). That all four manganese ions are in oxidation state +2 is confirmed by the bond lengths and by the presence of two counter-ions per complex cation. Sections of the aromatic ligands overlap resulting in π -stacking interactions which, although not necessarily a controlling factor in the structure, must provide some additional degree of stabilisation. The relative ease with which the ligands L¹ can distort from planarity by the introduction of twists between the bipyridyl and phenolate segments of each ligand L¹ allows these stacking interactions to be optimised. In all six ligands the bipyridyl fragment is nearly planar (the torsion angles within the bipyridyl fragments are all < 4°) whereas the phenolate ring is substantially twisted away from the plane of its neighbouring pyridyl ring (torsion angles 25–40°). Apart from being necessary on the grounds that the phenolate oxygen atom is formally sp³ hybridised, this results in π overlap between aromatic rings 7 and 12, and 10 and 13. The geometry around each six-co-ordinate Mn^{II} ion is far more irregular than those observed in the binuclear copper(II) (elongated square pyramidal) and nickel(II) (octahedral) complexes,^{6,9} which suggests that the ability of Mn^{II} to tolerate a distorted co-ordination environment is an important factor in the formation of this

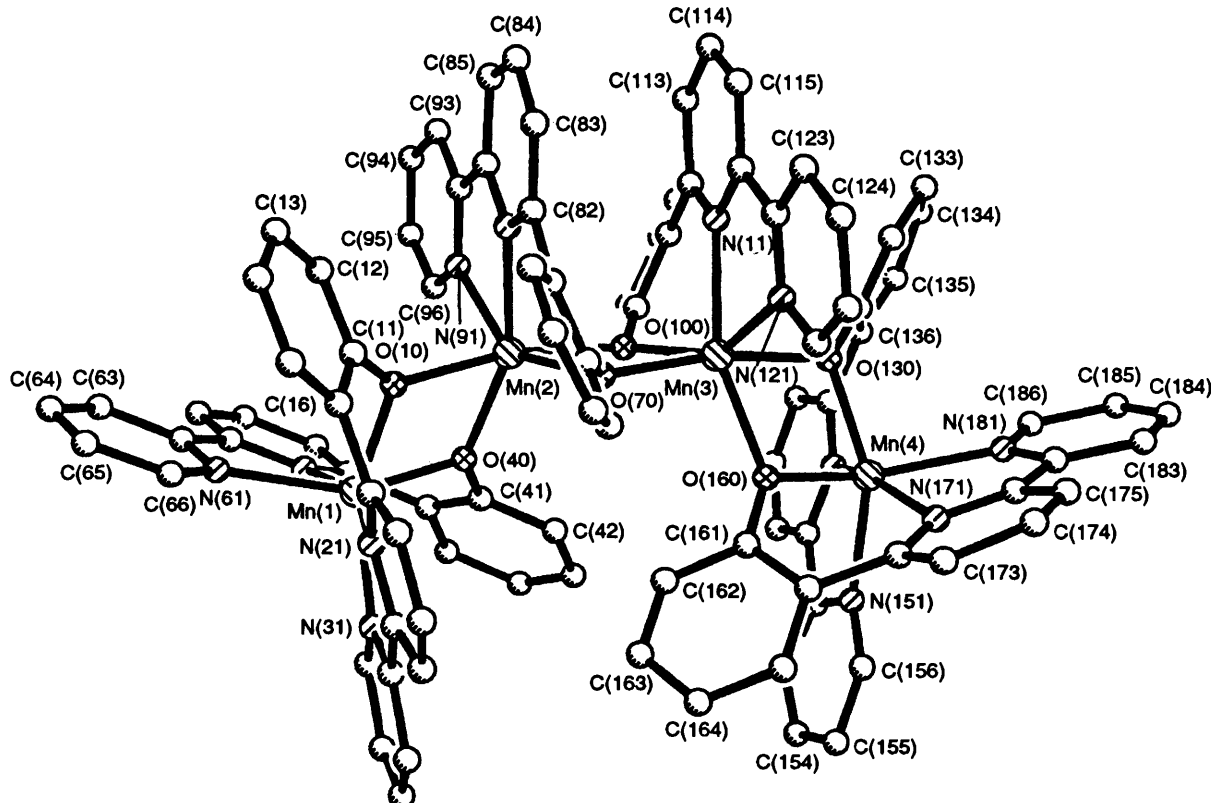


Fig. 3 Crystal structure of the cation of **3**

Table 6 Atomic coordinates ($\times 10^4$) for **2** with e.s.d.s in parentheses

Atom	<i>x</i>	<i>y</i>	<i>z</i>	Atom	<i>x</i>	<i>y</i>	<i>z</i>
Cd(1)	2 923(1)	9 809(1)	3 040(1)	C(93)	3 898(3)	14 033(9)	2 792(4)
Cd(2)	2 534(1)	12 754(1)	2 555(1)	C(94)	4 025(3)	13 305(11)	2 480(4)
O(1)	1 916(2)	12 510(5)	2 696(2)	C(95)	3 736(3)	12 447(9)	2 162(4)
C(1)	1 936(3)	12 194(8)	3 102(4)	C(96)	3 321(3)	12 348(8)	2 177(3)
N(1)	1 578(3)	12 103(6)	3 205(3)	B(100)	4 265(2)	8 668(8)	960(3)
C(1A)	1 635(5)	11 734(11)	3 702(5)	C(111)	4 426(2)	8 062(7)	547(3)
C(1B)	1 132(3)	12 373(10)	2 818(5)	C(112)	4 467(2)	8 782(8)	173(3)
O(2)	2 113(2)	13 553(5)	1 780(2)	C(113)	4 593(3)	8 320(11)	-186(3)
C(2)	1 716(3)	13 378(8)	1 533(3)	C(114)	4 676(3)	7 097(12)	-203(3)
N(2)	1 454(2)	14 076(6)	1 161(2)	C(115)	4 644(2)	6 345(9)	159(3)
C(2A)	1 630(4)	15 179(10)	1 032(4)	C(116)	4 530(2)	6 825(8)	528(3)
C(2B)	979(3)	13 852(9)	890(3)	C(121)	3 708(2)	8 795(7)	717(3)
O(10)	2 987(1)	11 759(4)	3 286(2)	C(122)	3 466(3)	8 642(9)	1 001(3)
C(11)	3 325(2)	12 042(6)	3 721(3)	C(123)	2 996(3)	8 849(11)	795(5)
C(12)	3 234(2)	12 702(7)	4 081(3)	C(124)	2 782(3)	9 236(10)	332(5)
C(13)	3 570(3)	13 008(8)	4 543(3)	C(125)	3 010(3)	9 411(9)	38(4)
C(14)	4 005(3)	12 667(9)	4 657(3)	C(126)	3 467(2)	9 184(7)	229(3)
C(15)	4 100(2)	12 050(8)	4 312(3)	C(131)	4 475(2)	10 049(7)	1 099(2)
C(16)	3 777(2)	11 716(6)	3 839(3)	C(132)	4 228(3)	11 083(8)	1 104(3)
N(21)	3 678(2)	10 121(5)	3 210(2)	C(133)	4 410(4)	12 268(9)	1 192(3)
C(22)	3 929(2)	11 045(7)	3 503(3)	C(134)	4 852(4)	12 430(9)	1 291(3)
C(23)	4 343(2)	11 313(7)	3 498(3)	C(135)	5 107(3)	11 437(10)	1 302(3)
C(24)	4 486(2)	10 638(8)	3 203(3)	C(136)	4 918(2)	10 297(8)	1 203(3)
C(25)	4 233(2)	9 686(7)	2 914(3)	C(141)	4 416(2)	7 811(7)	1 465(2)
C(26)	3 827(2)	9 462(7)	2 923(3)	C(142)	4 244(2)	6 642(7)	1 449(3)
N(31)	3 134(2)	8 352(5)	2 620(2)	C(143)	4 368(3)	5 884(8)	1 862(4)
C(32)	3 536(2)	8 446(6)	2 615(3)	C(144)	4 669(3)	6 271(9)	2 324(3)
C(33)	3 672(3)	7 634(8)	2 343(3)	C(145)	4 840(2)	7 433(9)	2 359(3)
C(34)	3 386(3)	6 732(9)	2 066(3)	C(146)	4 716(2)	8 169(7)	1 943(3)
C(35)	2 976(3)	6 638(8)	2 068(3)	B(200)	366(2)	8 822(7)	3 843(3)
C(36)	2 861(3)	7 460(7)	2 345(3)	C(211)	91(3)	7 635(6)	3 928(3)
O(40)	2 483(1)	10 780(4)	2 327(2)	C(212)	-302(3)	7 185(8)	3 560(3)
C(41)	2 180(2)	10 114(7)	1 961(3)	C(213)	-562(4)	6 260(10)	3 625(5)
C(42)	2 163(3)	10 195(8)	1 473(3)	C(214)	-417(5)	5 769(9)	4 107(6)
C(43)	1 872(3)	9 513(9)	1 084(3)	C(215)	-46(5)	6 207(10)	4 491(5)
C(44)	1 587(3)	8 724(9)	1 165(3)	C(216)	207(3)	7 114(8)	4 399(4)
C(45)	1 582(2)	8 638(7)	1 626(3)	C(221)	337(2)	8 807(6)	3 274(2)
C(46)	1 874(2)	9 327(6)	2 041(3)	C(222)	335(2)	9 880(7)	3 006(3)
N(51)	2 222(2)	9 121(5)	2 960(2)	C(223)	298(2)	9 859(8)	2 510(3)
C(52)	1 846(2)	9 173(6)	2 525(3)	C(224)	265(2)	8 775(10)	2 264(3)
C(53)	1 432(2)	9 038(7)	2 545(3)	C(225)	288(2)	7 709(8)	2 520(3)
C(54)	1 402(2)	8 797(7)	2 987(3)	C(226)	323(2)	7 723(7)	3 011(3)
C(55)	1 786(2)	8 720(6)	3 424(3)	C(231)	112(2)	10 003(6)	3 953(2)
C(56)	2 191(2)	8 909(6)	3 397(3)	C(232)	209(2)	10 371(7)	4 448(3)
N(61)	2 995(2)	9 124(5)	3 809(2)	C(233)	-7(2)	11 320(7)	4 667(3)
C(62)	2 616(2)	8 871(6)	3 863(3)	C(234)	-338(3)	11 968(7)	4 191(3)
C(63)	2 620(3)	8 575(9)	4 317(3)	C(235)	-450(2)	11 634(7)	3 701(3)
C(64)	3 027(3)	8 535(10)	4 736(3)	C(236)	-234(2)	10 656(7)	3 592(3)
C(65)	3 411(3)	8 821(9)	4 691(4)	C(241)	892(2)	8 794(7)	4 216(2)
C(66)	3 386(2)	9 097(8)	4 225(4)	C(242)	1 143(3)	7 728(9)	4 347(3)
O(70)	2 223(2)	15 070(7)	3 871(2)	C(243)	1 593(3)	7 684(12)	4 661(4)
C(71)	1 989(3)	15 309(7)	3 376(3)	C(244)	1 813(3)	8 737(15)	4 844(4)
C(72)	1 534(3)	15 448(8)	3 172(3)	C(245)	1 596(3)	9 845(11)	4 714(3)
C(73)	1 304(3)	15 616(9)	2 663(4)	C(246)	1 133(1)	9 832(3)	4 392(2)
C(74)	1 524(3)	15 626(8)	2 351(4)	O(900)	1 605(1)	14 529(3)	4 256(2)
C(75)	1 972(3)	15 502(7)	2 553(3)	C(900)	1 505(1)	14 205(3)	4 609(2)
C(76)	2 218(2)	15 329(6)	3 069(3)	N(900)	1 104(1)	13 972(3)	4 489(2)
N(81)	2 870(2)	14 569(5)	2 972(2)	C(901)	704(1)	14 027(3)	4 027(2)
C(82)	2 721(2)	15 245(7)	3 259(3)	C(902)	1 003(1)	13 619(3)	4 909(2)
C(83)	3 001(3)	15 897(7)	3 684(3)	O(800)	2 116(1)	12 592(3)	5 610(2)
C(84)	3 452(3)	15 870(9)	3 811(4)	C(800)	2 472(1)	12 203(3)	5 742(2)
C(85)	3 612(3)	15 213(9)	3 524(3)	N(800)	2 821(1)	11 677(3)	5 615(2)
C(86)	3 320(2)	14 582(7)	3 115(3)	C(801)	3 039(1)	10 593(3)	5 932(2)
N(91)	3 199(2)	13 038(6)	2 470(2)	C(802)	2 791(1)	12 050(3)	5 127(2)
C(92)	3 478(2)	13 872(7)	2 787(3)				

tetranuclear structure: for example, those co-ordination-sphere bond angles which would be 90° in a regular octahedron vary from 72 to 118° around the Mn centres of **3**.

High-nuclearity complexes of manganese in various oxidation states are currently receiving much attention, both as models for manganese-containing metalloproteins such as catalases¹⁵

and the water-oxidising centre of photosystem II,¹⁶ and for their unusual magnetic properties such as very high magnetic moments,¹⁷ ferromagnetic or antiferromagnetic exchange¹⁸ and spin frustration.¹⁹ The magnetic properties of **3** will be reported later, but for now we note that the structurally similar complex $[\text{Mn}_4\text{L}^2_6][\text{ClO}_4]_2$ undergoes ferromagnetic exchange

Table 7 Selected bond lengths (\AA) and angles ($^\circ$) for **3** with e.s.d.s in parentheses

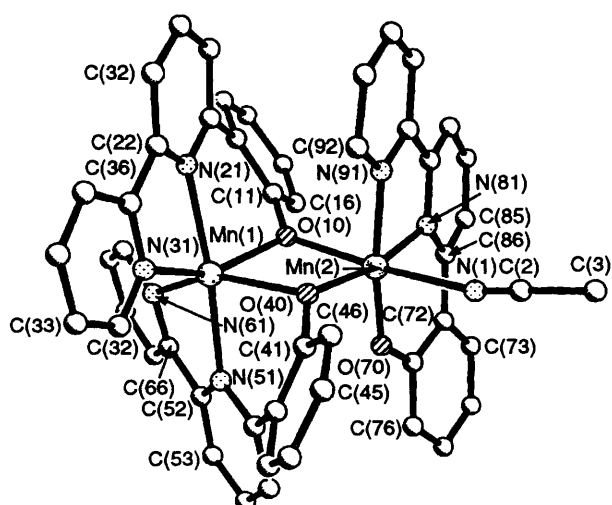
Mn(1)–O(10)	2.085(6)	Mn(2)–O(70)	2.116(6)	Mn(3)–O(100)	2.103(6)	Mn(4)–O(130)	2.073(7)
Mn(1)–O(40)	2.124(6)	Mn(2)–O(10)	2.162(6)	Mn(3)–O(160)	2.156(6)	Mn(4)–O(160)	2.095(7)
Mn(1)–N(31)	2.239(8)	Mn(2)–O(40)	2.160(6)	Mn(3)–O(70)	2.162(7)	Mn(4)–N(181)	2.241(10)
Mn(1)–N(61)	2.250(8)	Mn(2)–O(100)	2.184(6)	Mn(3)–O(130)	2.192(7)	Mn(4)–N(151)	2.279(10)
Mn(1)–N(21)	2.313(8)	Mn(2)–N(91)	2.221(8)	Mn(3)–N(121)	2.252(8)	Mn(4)–N(171)	2.282(10)
Mn(1)–N(51)	2.318(8)	Mn(2)–N(81)	2.302(8)	Mn(3)–N(111)	2.272(8)	Mn(4)–N(141)	2.291(10)
O(10)–Mn(1)–O(40)	76.8(2)	O(70)–Mn(2)–O(10)	100.8(2)	O(100)–Mn(3)–O(160)	112.1(3)	O(130)–Mn(4)–O(160)	77.7(3)
O(10)–Mn(1)–N(31)	145.3(3)	O(70)–Mn(2)–O(40)	114.2(3)	O(100)–Mn(3)–O(70)	77.4(2)	O(130)–Mn(4)–N(181)	96.3(3)
O(40)–Mn(1)–N(31)	98.1(3)	O(10)–Mn(2)–O(40)	74.4(2)	O(160)–Mn(3)–O(70)	96.6(2)	O(160)–Mn(4)–N(181)	144.2(4)
O(10)–Mn(1)–N(61)	95.6(3)	O(70)–Mn(2)–O(100)	76.7(2)	O(100)–Mn(3)–O(130)	103.1(3)	O(130)–Mn(4)–N(151)	147.0(4)
O(40)–Mn(1)–N(61)	145.2(3)	O(10)–Mn(2)–O(100)	169.3(2)	O(160)–Mn(3)–O(130)	73.9(2)	O(160)–Mn(4)–N(151)	95.9(3)
N(31)–Mn(1)–N(61)	106.1(3)	O(40)–Mn(2)–O(100)	96.9(2)	O(70)–Mn(3)–O(130)	170.1(3)	N(181)–Mn(4)–N(151)	106.5(4)
O(10)–Mn(1)–N(21)	80.3(3)	O(70)–Mn(2)–N(91)	145.7(3)	O(100)–Mn(3)–N(121)	147.6(3)	O(130)–Mn(4)–N(171)	116.4(3)
O(40)–Mn(1)–N(21)	117.6(3)	O(10)–Mn(2)–N(91)	98.4(3)	O(160)–Mn(3)–N(121)	98.5(3)	O(160)–Mn(4)–N(171)	79.7(3)
N(31)–Mn(1)–N(21)	71.7(3)	O(40)–Mn(2)–N(91)	98.2(3)	O(70)–Mn(3)–N(121)	88.8(3)	N(181)–Mn(4)–N(171)	71.5(4)
N(61)–Mn(1)–N(21)	93.8(3)	O(100)–Mn(2)–N(91)	88.9(3)	O(130)–Mn(3)–N(121)	95.4(3)	N(151)–Mn(4)–N(171)	93.6(4)
O(10)–Mn(1)–N(51)	112.6(3)	O(70)–Mn(2)–N(81)	80.2(3)	O(100)–Mn(3)–N(111)	81.2(3)	O(130)–Mn(4)–N(141)	80.1(4)
O(40)–Mn(1)–N(51)	79.7(3)	O(10)–Mn(2)–N(81)	88.5(3)	O(160)–Mn(3)–N(111)	159.4(3)	O(160)–Mn(4)–N(141)	113.8(3)
N(31)–Mn(1)–N(51)	99.8(3)	O(40)–Mn(2)–N(81)	159.2(3)	O(70)–Mn(3)–N(111)	101.8(3)	N(181)–Mn(4)–N(141)	99.5(4)
N(61)–Mn(1)–N(51)	72.0(3)	O(100)–Mn(2)–N(81)	101.1(3)	O(130)–Mn(3)–N(111)	88.1(3)	N(151)–Mn(4)–N(141)	72.9(4)
N(21)–Mn(1)–N(51)	161.2(3)	N(91)–Mn(2)–N(81)	72.2(3)	N(121)–Mn(3)–N(111)	73.0(3)	N(171)–Mn(4)–N(141)	161.4(3)

Table 8 Atomic coordinates ($\times 10^4$) for **3** with e.s.d.s in parentheses

Atom	<i>x</i>	<i>y</i>	<i>z</i>	Atom	<i>x</i>	<i>y</i>	<i>z</i>
Mn(1)	2 301(1)	2 497(1)	3 137(1)	C(116)	-3 096(7)	5 976(7)	3 091(4)
Mn(2)	-81(1)	3 628(1)	3 091(1)	N(121)	-1 936(6)	6 393(5)	2 589(3)
Mn(3)	-1 359(1)	5 099(1)	2 382(1)	C(122)	-2 638(8)	6 579(6)	2 935(4)
Mn(4)	-1 370(1)	5 424(1)	1 252(1)	C(123)	-2 942(10)	7 308(8)	3 127(5)
O(10)	1 127(4)	3 352(4)	3 494(2)	C(124)	-2 500(12)	7 854(9)	2 962(5)
C(11)	1 247(7)	3 689(6)	3 850(3)	C(125)	-1 787(11)	7 665(8)	2 607(5)
C(12)	695(8)	3 657(7)	4 264(3)	C(126)	-1 547(9)	6 921(6)	2 435(4)
C(13)	782(10)	4 005(10)	4 637(4)	O(130)	-2 283(5)	5 331(4)	1 827(2)
C(14)	1 464(11)	4 376(10)	4 620(4)	C(131)	-3 173(8)	5 306(9)	1 805(4)
C(15)	2 009(10)	4 408(8)	4 227(4)	C(132)	-3 973(9)	5 870(12)	2 028(5)
C(16)	1 939(7)	4 075(7)	3 830(3)	C(133)	-4 884(14)	5 874(15)	2 005(6)
N(21)	2 907(6)	3 532(5)	3 120(3)	C(134)	-4 942(15)	5 268(19)	1 763(7)
C(22)	2 571(8)	4 143(7)	3 415(4)	C(135)	-4 208(17)	4 741(15)	1 515(6)
C(23)	2 882(9)	4 811(7)	3 323(5)	C(136)	-3 227(12)	4 708(12)	1 535(5)
C(24)	3 515(9)	4 842(8)	2 957(4)	N(141)	-1 638(9)	4 282(6)	1 107(3)
C(25)	3 835(9)	4 221(8)	2 661(4)	C(142)	-2 409(14)	4 094(11)	1 291(5)
C(26)	3 528(7)	3 564(7)	2 757(3)	C(143)	-2 460(22)	3 341(15)	1 266(7)
N(31)	3 490(6)	2 311(6)	2 566(3)	C(144)	-1 706(24)	2 794(14)	1 007(9)
C(32)	3 886(8)	2 876(7)	2 463(3)	C(145)	-890(20)	2 978(11)	810(6)
C(33)	4 578(9)	2 833(9)	2 100(4)	C(146)	-845(14)	3 728(8)	857(5)
C(34)	4 893(9)	2 182(10)	1 842(4)	N(151)	-153(8)	4 759(6)	723(3)
C(35)	4 507(10)	1 569(10)	1 938(4)	C(152)	-41(12)	4 020(9)	672(4)
C(36)	3 796(9)	1 655(8)	2 312(4)	C(153)	783(18)	3 423(12)	439(5)
O(40)	1 122(5)	2 689(4)	2 748(2)	C(154)	1 432(16)	3 761(14)	286(5)
C(41)	1 271(7)	2 193(6)	2 407(3)	C(155)	1 397(12)	4 552(14)	309(5)
C(42)	1 057(9)	2 533(8)	1 977(4)	C(156)	546(9)	5 018(10)	549(4)
C(43)	1 253(12)	2 084(9)	1 598(4)	O(160)	-469(4)	5 244(4)	1 771(2)
C(44)	1 618(12)	1 263(10)	1 656(5)	C(161)	404(7)	5 292(6)	1 685(3)
C(45)	1 822(11)	889(9)	2 088(5)	C(162)	1 244(8)	4 646(8)	1 816(4)
C(46)	1 618(8)	1 363(6)	2 467(4)	C(163)	2 167(10)	4 648(11)	1 721(5)
N(51)	2 206(6)	1 215(5)	3 214(3)	C(164)	2 329(11)	5 281(14)	1 477(5)
C(52)	1 830(8)	926(6)	2 917(4)	C(165)	1 528(12)	5 960(11)	1 345(5)
C(53)	1 639(11)	208(7)	3 035(5)	C(166)	552(9)	5 964(8)	1 437(4)
C(54)	1 854(11)	-184(8)	3 447(6)	N(171)	-1 024(7)	6 586(5)	1 147(3)
C(55)	2 258(10)	108(8)	3 740(5)	C(172)	-281(11)	6 699(8)	1 295(4)
C(56)	2 419(8)	819(7)	3 612(4)	C(173)	-271(15)	7 494(10)	1 326(5)
N(61)	3 037(6)	1 845(5)	3 753(3)	C(174)	-1 137(19)	8 139(9)	1 180(6)
C(62)	2 863(8)	1 161(7)	3 897(4)	C(175)	-1 829(17)	7 982(12)	1 013(6)
C(63)	3 113(10)	824(8)	4 336(4)	C(176)	-1 748(13)	7 220(8)	1 012(4)
C(64)	3 548(11)	1 177(8)	4 595(5)	N(181)	-2 530(7)	6 359(8)	871(3)
C(65)	3 739(9)	1 861(8)	4 428(4)	C(182)	-2 530(11)	7 104(9)	817(4)
C(66)	3 473(8)	2 171(7)	4 001(4)	C(183)	-3 284(16)	7 720(11)	577(6)
O(70)	-240(5)	4 822(4)	2 837(2)	C(184)	-3 976(19)	7 522(17)	411(7)
C(71)	-59(8)	5 319(7)	3 079(4)	C(185)	-3 975(12)	6 768(16)	457(6)
C(72)	531(10)	5 741(7)	2 886(5)	C(186)	-3 199(10)	6 168(11)	707(4)
C(73)	705(12)	6 285(8)	3 145(6)	B(200)	5 760(9)	2 277(7)	5 307(4)
C(74)	353(12)	6 396(9)	3 585(6)	C(211)	4 841(9)	2 023(7)	5 521(3)
C(75)	-231(12)	5 998(9)	3 781(5)	C(212)	3 880(9)	2 495(8)	5 471(4)

Table 8 (continued)

Atom	<i>x</i>	<i>y</i>	<i>z</i>	Atom	<i>x</i>	<i>y</i>	<i>z</i>
C(76)	-476(8)	5 988(9)	3 530(4)	C(213)	3 069(10)	2 277(9)	5 634(5)
N(81)	-1 099(6)	4 351(5)	3 677(3)	C(214)	3 246(13)	1 527(11)	5 870(5)
C(82)	-1 161(8)	5 105(7)	3 769(3)	C(215)	4 157(13)	1 053(10)	5 927(5)
C(83)	-1 853(11)	5 504(9)	4 108(5)	C(216)	4 984(10)	1 272(8)	5 763(4)
C(84)	-2 475(12)	5 174(12)	4 331(6)	C(221)	6 661(8)	1 473(6)	5 097(4)
C(85)	-2 426(10)	4 416(11)	4 256(4)	C(222)	6 476(10)	946(7)	4 827(4)
C(86)	-1 693(8)	3 983(8)	3 911(4)	C(223)	7 209(13)	294(7)	4 630(4)
N(91)	-815(6)	2 841(5)	3 479(3)	C(224)	8 163(13)	123(9)	4 704(5)
C(92)	-1 540(8)	3 169(8)	3 806(3)	C(225)	8 377(11)	592(9)	4 961(5)
C(93)	-2 097(11)	2 758(10)	4 034(5)	C(226)	7 628(9)	1 263(7)	5 149(4)
C(94)	-1 872(13)	1 978(12)	3 933(6)	C(231)	6 195(7)	2 608(6)	5 704(4)
C(95)	-1 171(11)	1 614(9)	3 597(5)	C(232)	6 130(9)	2 355(8)	6 152(4)
C(96)	-640(9)	2 090(8)	3 378(5)	C(233)	6 557(10)	2 613(8)	6 479(5)
O(100)	-1 094(4)	3 871(4)	2 576(2)	C(234)	7 066(12)	3 108(8)	6 356(5)
C(101)	-1 774(8)	3 552(7)	2 563(4)	C(235)	7 175(10)	3 360(8)	5 914(5)
C(102)	-1 501(10)	2 807(7)	2 353(5)	C(236)	6 734(10)	3 129(7)	5 591(5)
C(103)	-2 194(13)	2 452(9)	2 342(6)	C(241)	5 420(8)	2 989(6)	4 902(4)
C(104)	-3 136(12)	2 848(11)	2 509(6)	C(242)	4 936(8)	3 794(6)	5 005(4)
C(105)	-3 389(11)	3 538(9)	2 718(5)	C(243)	4 522(8)	4 421(7)	4 676(5)
C(106)	-2 738(8)	3 923(7)	2 739(4)	C(244)	4 615(9)	4 238(8)	4 230(4)
N(111)	-2 714(6)	5 255(5)	2 874(3)	C(245)	5 088(9)	3 456(8)	4 118(4)
C(112)	-3 120(8)	4 690(8)	2 982(4)	C(246)	5 495(8)	2 841(7)	4 450(4)
C(113)	-3 908(10)	4 823(10)	3 317(5)	B(300)	3 155(11)	8 949(9)	9 459(5)
C(114)	-4 282(12)	5 560(11)	3 534(5)	C(311)	2 209(12)	8 719(8)	9 641(5)
C(115)	-3 865(10)	6 132(9)	3 413(4)	C(312)	1 282(11)	9 173(9)	9 516(6)
C(313)	458(14)	9 047(11)	9 708(7)	C(346)	4 207(11)	7 384(7)	9 352(4)
C(314)	479(15)	8 495(12)	10 034(7)	C(901)	10 253(32)	-1 427(22)	3 881(14)
C(315)	1 368(15)	8 033(12)	10 197(5)	C(902)	10 018(33)	-1 911(20)	4 264(13)
C(316)	2 236(13)	8 148(11)	9 993(5)	O(903)	10 045(20)	-1 688(18)	4 666(11)
C(321)	3 227(10)	9 571(8)	9 831(5)	C(904)	9 981(42)	-2 293(26)	4 942(15)
C(322)	3 919(18)	9 434(13)	10 105(7)	C(905)	9 711(23)	-1 718(19)	5 382(12)
C(323)	3 908(19)	9 972(16)	10 428(8)	O(911)	5 000	5 000	10 000
C(324)	3 149(15)	10 641(14)	10 482(6)	C(912)	3 929(22)	5 679(19)	10 310(11)
C(325)	2 451(13)	10 835(10)	10 250(7)	C(913)	3 367(8)	5 621(6)	10 068(4)
C(326)	2 462(11)	10 312(8)	9 905(5)	C(921)	-5 619(8)	8 490(6)	1 800(4)
C(331)	3 052(10)	9 413(7)	8 955(4)	C(922)	-5 361(8)	8 706(6)	2 211(4)
C(332)	3 465(10)	9 985(9)	8 814(5)	O(923)	-5 316(8)	8 885(6)	2 686(4)
C(333)	3 457(13)	10 361(11)	8 361(6)	C(924)	-5 236(8)	9 362(6)	2 878(4)
C(334)	3 044(14)	10 090(10)	8 069(6)	C(925)	-4 964(8)	9 900(6)	2 986(4)
C(335)	2 650(15)	9 498(11)	8 163(6)	C(931)	-3 822(8)	10 954(6)	3 201(4)
C(336)	2 656(12)	9 171(8)	8 615(5)	C(932)	-2 780(8)	10 198(6)	3 212(4)
C(341)	4 166(9)	8 169(7)	9 388(4)	N(933)	-1 742(8)	9 775(6)	3 201(4)
C(342)	5 082(10)	8 248(8)	9 313(5)	C(941)	40(8)	9 776(6)	1 820(4)
C(343)	5 937(11)	7 608(9)	9 214(5)	C(942)	604(8)	9 475(6)	1 321(4)
C(344)	5 927(12)	6 850(9)	9 194(5)	N(943)	1 440(8)	9 298(6)	1 001(4)
C(345)	5 041(12)	6 724(9)	9 254(5)				

**Fig. 4** Crystal structure of the cation of **4**

at low temperatures, with the magnetic moment reaching $7.3 \mu_B$ per Mn^{II} at 4 K.⁴ We could not obtain an EPR spectrum of **3** at either room temperature or at 77 K, which suggests that magnetic exchange processes are providing efficient relaxation and the signal is broadened to the extent that it cannot be detected.

Complex 4.—Reaction of HL^1 with manganese(III) acetate in air afforded a dark brown solution, from which a dark brown solid precipitated on addition of aqueous KPF_6 . The FAB mass spectrum of the precipitate showed peaks at m/z 851, 550 and 302, which correspond respectively to $\{Mn_2L^{1_3}\}$, $\{MnL^{1_2}\}$ and $\{MnL^1\}$; this spectrum is very similar to that of complex **3**. Crystals were grown from acetonitrile-diethyl ether and the X-ray structure (Fig. 4, Tables 9 and 10) shows the complex to be $[Mn_2L^{1_3}(MeCN)]PF_6 \cdot Et_2O$ (**4**· Et_2O). It is a mixed-valence $Mn^{II}Mn^{III}$ complex, as confirmed by the presence of two anions and the bond lengths at the two metal centres. The Mn^{II} ion [$Mn(1)$] is in a typical distorted N_4O_2 -octahedral geometry, co-ordinated by two ligands L^1 of which the two *cis*-oriented phenolates bridge to the Mn^{III} ion [$Mn(2)$]. Ion $Mn(2)$ has, in addition to the two shared phenolate donors, one molecule of

L^1 , and a molecule of acetonitrile (from the recrystallisation solvent) resulting in a *fac*- N_3O_3 co-ordination environment.

Table 9 Selected bond lengths (\AA) and angles ($^\circ$) for **4** with e.s.d.s in parentheses

Mn(1)–O(10)	2.088(4)	Mn(2)–O(70)	1.832(4)
Mn(1)–N(31)	2.194(5)	Mn(2)–O(40)	1.924(4)
Mn(1)–N(61)	2.229(5)	Mn(2)–N(81)	2.015(5)
Mn(1)–N(51)	2.225(5)	Mn(2)–N(91)	2.038(5)
Mn(1)–O(40)	2.239(4)	Mn(2)–O(10)	2.143(4)
Mn(1)–N(21)	2.245(5)	Mn(2)–N(1)	2.390(6)
O(10)–Mn(1)–N(31)	148.1(2)	O(70)–Mn(2)–O(40)	94.2(2)
O(10)–Mn(1)–N(61)	90.7(2)	O(70)–Mn(2)–N(81)	93.3(2)
N(31)–Mn(1)–N(61)	114.2(2)	O(40)–Mn(2)–N(81)	167.8(2)
O(10)–Mn(1)–N(51)	102.2(2)	O(70)–Mn(2)–N(91)	172.3(2)
N(31)–Mn(1)–N(51)	103.7(2)	O(40)–Mn(2)–N(91)	92.7(2)
N(61)–Mn(1)–N(51)	74.2(2)	N(81)–Mn(2)–N(91)	80.5(2)
O(10)–Mn(1)–O(40)	74.75(14)	O(70)–Mn(2)–O(10)	97.6(2)
N(31)–Mn(1)–O(40)	91.3(2)	O(40)–Mn(2)–O(10)	80.4(2)
N(61)–Mn(1)–O(40)	147.6(2)	N(81)–Mn(2)–O(10)	89.0(2)
N(51)–Mn(1)–O(40)	80.8(2)	N(91)–Mn(2)–O(10)	86.9(2)
O(10)–Mn(1)–N(21)	81.9(2)	O(70)–Mn(2)–N(1)	90.3(2)
N(31)–Mn(1)–N(21)	74.1(2)	O(40)–Mn(2)–N(1)	94.8(2)
N(61)–Mn(1)–N(21)	101.3(2)	N(81)–Mn(2)–N(1)	94.8(2)
N(51)–Mn(1)–N(21)	173.8(2)	N(91)–Mn(2)–N(1)	85.7(2)
O(40)–Mn(1)–N(21)	104.9(2)	O(10)–Mn(2)–N(1)	171.0(2)
C(2)–N(1)–Mn(2)	167.2(6)	Mn(1)–O(10)–Mn(2)	101.0(2)
Mn(2)–O(40)–Mn(1)	103.1(2)		

The bonds to Mn(1) are appreciably longer than those to Mn(2): for example, the Mn(1)–N(pyridyl) bond lengths lie in the range 2.19–2.25 \AA whereas the Mn(2)–N(pyridyl) bond lengths are 2.038 and 2.015 \AA . The N(1)–Mn(2)–O(10) axis is *ca.* 16% longer than the other two, arising from a Jahn–Teller distortion typical of high-spin Mn^{III} centres. The Mn₂(μ -O)₂ bridge is therefore asymmetric, with alternating short/long Mn–O distances around the four-membered ring. Again the typical stacking between sections of the aromatic ligands on adjacent metal ions is evident (*e.g.* ring 2 and ring 9, separated by *ca.* 3.5 \AA). The structure of **4** is similar to that of the binuclear cadmium(II) complex **2**, with the exception that the pendant phenol in **2**, co-ordination of which would result in too much electron density around a 2+ metal centre, does co-ordinate to the 3+ metal centre of **4**.

Comparison of this structure with that of the tetranuclear complex **3** is interesting, as it shows how the metal oxidation state controls the degree of aggregation. Manganese(III) has a strong stereoelectronic preference for an elongated tetragonal geometry, and the higher charge on the Mn^{III} centre compared to Mn^{II} is capable of supporting a terminal phenolate donor without having to share the electron density by bridging. Both of these factors mitigate against formation of a tetranuclear species similar to that of **3**: the Mn^{III} ions would be required both to share phenolate ligands, and to tolerate an irregular geometry. If the Mn^{III} ions were reduced to Mn^{II} one can see how loss of MeCN ligands could be followed by dimerisation/bridge formation to give **3**. However electrochemical examination

Table 10 Atomic coordinates ($\times 10^4$) for **4** with e.s.d.s in parentheses

Atom	x	y	z	Atom	x	y	z
Mn(1)	2 535(1)	2 192(1)	1 761(1)	C(65)	3 738(6)	306(4)	2 791(2)
Mn(2)	4 775(1)	2 726(1)	1 280(1)	C(66)	3 403(5)	1 030(3)	2 572(2)
N(1)	5 646(5)	3 956(3)	1 090(2)	O(70)	5 809(4)	2 674(3)	1 847(2)
C(2)	5 929(7)	4 436(5)	936(3)	C(71)	6 857(5)	2 331(3)	1 950(2)
C(3)	6 406(9)	5 167(5)	705(4)	C(72)	7 373(6)	1 851(4)	1 632(3)
O(10)	3 746(3)	1 693(2)	1 383(1)	C(73)	8 483(7)	1 538(5)	1 803(3)
C(11)	3 558(6)	971(3)	1 183(2)	C(74)	9 090(7)	1 698(5)	2 248(4)
C(12)	2 488(6)	755(4)	894(2)	C(75)	8 596(6)	2 173(4)	2 561(3)
C(13)	2 350(8)	–33(4)	718(3)	C(76)	7 477(6)	2 482(4)	2 408(2)
C(14)	3 247(9)	–587(4)	803(3)	N(81)	5 778(5)	2 026(3)	939(2)
C(15)	4 309(9)	–360(4)	1 064(2)	C(82)	5 258(8)	1 836(4)	485(2)
C(16)	4 468(7)	399(4)	1 259(2)	C(83)	5 707(10)	1 238(6)	234(3)
N(21)	1 276(4)	1 865(3)	1 094(2)	C(84)	6 687(11)	857(6)	434(4)
C(22)	349(6)	2 365(4)	982(2)	C(85)	7 230(9)	1 045(5)	881(3)
C(23)	–355(7)	2 357(6)	530(3)	C(86)	6 775(7)	1 647(4)	1 147(2)
C(24)	–106(8)	1 821(6)	198(3)	N(91)	3 819(5)	2 785(3)	608(2)
C(25)	832(8)	1 304(5)	309(3)	C(92)	2 858(7)	3 240(5)	472(3)
C(26)	1 504(6)	1 327(4)	765(2)	C(93)	2 271(9)	3 228(6)	3(3)
N(31)	981(4)	2 948(3)	1 754(2)	C(94)	2 632(11)	2 731(6)	–309(3)
C(32)	849(6)	3 448(4)	2 114(3)	C(95)	3 573(10)	2 245(6)	–176(3)
C(33)	–111(8)	3 952(5)	2 084(4)	C(96)	4 188(7)	2 301(4)	294(2)
C(34)	–944(9)	3 935(6)	1 681(4)	P(1)	6 783(3)	3 497(2)	–360(1)
C(35)	–840(7)	3 422(5)	1 314(3)	F(1)	6 704(13)	4 422(6)	–387(5)
C(36)	169(6)	2 937(4)	1 355(3)	F(2)	7 165(14)	2 648(6)	–353(5)
O(40)	3 557(3)	3 233(2)	1 553(1)	F(3)	6 820(15)	3 618(8)	–871(3)
C(41)	3 530(5)	3 915(3)	1 820(2)	F(4)	6 282(18)	3 517(8)	45(4)
C(42)	3 745(5)	3 889(3)	2 319(2)	F(5)	5 664(9)	3 153(11)	–604(4)
C(43)	3 593(6)	4 598(4)	2 560(3)	F(6)	7 919(12)	3 709(8)	–121(7)
C(44)	3 248(6)	5 298(4)	2 332(3)	P(2)	1 052(4)	1 051(2)	–1 291(1)
C(45)	3 069(6)	5 325(4)	1 840(3)	F(7)	621(11)	1 594(7)	–942(4)
C(46)	3 215(6)	4 641(3)	1 586(2)	F(8)	92(15)	1 295(7)	–1 675(4)
N(51)	3 648(4)	2 452(3)	2 465(2)	F(9)	2 007(10)	841(6)	–884(4)
C(52)	3 962(5)	1 801(3)	2 742(2)	F(10)	493(8)	271(5)	–1 186(5)
C(53)	4 775(7)	1 853(4)	3 163(2)	F(11)	1 638(17)	519(6)	–1 604(5)
C(54)	5 284(7)	2 584(4)	3 297(2)	F(12)	1 721(15)	1 785(6)	–1 406(5)
C(55)	4 986(6)	3 246(4)	3 011(2)	C(501)	8 552(15)	6 259(11)	1 597(6)
C(56)	4 136(5)	3 166(3)	2 601(2)	C(502)	9 540(14)	6 259(11)	1 384(7)
N(61)	2 539(4)	1 071(3)	2 187(2)	O(503)	9 242(11)	5 696(8)	1 045(5)
C(62)	1 985(6)	393(4)	2 024(2)	C(504)	10 304(22)	5 631(22)	852(11)
C(63)	2 281(7)	–347(4)	2 228(3)	C(505)	10 071(27)	4 908(17)	468(12)
C(64)	3 176(7)	–387(4)	2 616(3)				

of **4** showed no evidence for a Mn^{III}–Mn^{II} couple at accessible potentials so we could not test this. Like **3**, complex **4** gave no EPR spectrum either at room temperature or at 77 K. Although Mn^{III} centres do not generally give EPR spectra at temperatures as high as 77 K due to their rapid relaxation, we might expect to see a signal from the Mn^{II} centre if the interaction between the two ions were negligible. The fact that the Mn^{II} centre is also invisible by EPR indicates the presence of magnetic exchange between the two centres; a magnetic study of **4** will be reported later.

Conclusion

The set of crystal structures described in this paper illustrates the fine balance that exists between the factors responsible for determining the structures of co-ordination complexes, which include the stereoelectronic requirements of the metal ion, the co-ordination modes available to the ligand, and non-covalent interactions such as hydrogen bonding and aromatic π stacking. These non-covalent interactions are particularly in evidence in some of these structures. It is noticeable that in complexes of first-row metal ions with a 2+ charge the negative charges on the phenolates are always shared in some way, usually by bridging to another metal ion, but also in other cases by bridging to a cationic boron fragment²⁰ or by being involved in hydrogen bonding, as in $[\{Ni_2L^1(HL^1)\}_2][PF_6]_2$.⁹ The relatively low charge on the metal is apparently too small to be comfortable with the concentration of negative charge provided by two anionic phenolates. In complexes of first-row metals with a 3+ charge (Cr, Co) simple mononuclear $[ML^1]_2^+$ complexes form. This may be because the higher 3+ charge is more appropriately stabilised by two phenolates, but may also be because bridging behaviour is electrostatically unfavourable since it requires 3+ metal centres to be brought close together instead of 2+ charges.

References

- D. A. Bardwell, D. Black, J. C. Jeffery, E. Schatz and M. D. Ward, *J. Chem. Soc., Dalton Trans.*, 1993, 2321 and refs. therein.
- J. P. Maher, P. H. Rieger, P. Thornton and M. D. Ward, *J. Chem. Soc., Dalton Trans.*, 1992, 3353; J. C. Jeffery, J. P. Maher, C. A. Otter, P. Thornton and M. D. Ward, *J. Chem. Soc., Dalton Trans.*, 1995, 819.
- D. A. Bardwell, J. C. Jeffery and M. D. Ward, *Inorg. Chim. Acta*, 1995, in the press.
- J. C. Jeffery, P. Thornton and M. D. Ward, *Inorg. Chem.*, 1994, **33**, 3612.
- J. M. Rawson and R. E. P. Winpenny, *Coord. Chem. Rev.*, 1995, **139**, 313.
- J. C. Jeffery, E. Schatz and M. D. Ward, *J. Chem. Soc., Dalton Trans.*, 1992, 1921.
- SHELXTL PLUS™ program system, Siemens Analytical X-Ray Instruments, Madison, WI, USA, 1989; SHELX 93 program system, Siemens Analytical X-Ray Instruments, Madison, WI, 1993.
- International Tables for X-Ray Crystallography*, Kynoch Press, Birmingham, 1974, vol. 4.
- B. M. Holligan, J. C. Jeffery and M. D. Ward, *J. Chem. Soc., Dalton Trans.*, 1992, 3337.
- K. Ozutsumi, K. Tohji, Y. Udagawa and S. Ishiguro, *Bull. Chem. Soc. Jpn.*, 1991, **64**, 1528; K. Ozutsumi, T. Takamuka, S. Ishiguro and H. Ohtaki, *Bull. Chem. Soc. Jpn.*, 1989, **62**, 1875; K. Ozutsumi, S. Ishiguro and H. Ohtaki, *Bull. Chem. Soc. Jpn.*, 1988, **61**, 945; K. Ozutsumi, S. Ishiguro and H. Ohtaki, *Bull. Chem. Soc. Jpn.*, 1988, **61**, 715.
- R. S. Drago, D. W. Meek, M. D. Joesten and L. LaRoche, *Inorg. Chem.*, 1963, **2**, 124; W. E. Bull, S. K. Madan and J. E. Willis, *Inorg. Chem.*, 1963, **2**, 303.
- M. Calligaris, G. Nardin, L. Randaccio and A. Ripamonti, *J. Chem. Soc. A*, 1970, 1069.
- S. S. Krishnamurthy and S. Soundararajan, *Can. J. Chem.*, 1969, **47**, 995.
- S. S. Tandon, S. Chander, L. K. Thompson, J. N. Bridson and V. McKee, *Inorg. Chim. Acta*, 1994, **219**, 55.
- R. M. Fronko and J. E. Penner-Hahn, *J. Am. Chem. Soc.*, 1988, **110**, 7554; G. S. Waldo, S. Yu and J. E. Penner-Hahn, *J. Am. Chem. Soc.*, 1992, **114**, 5869; H. Sakiyama, H. Okawa and R. Isobe, *J. Chem. Soc., Chem. Commun.*, 1993, 882.
- G. W. Brudvig, H. H. Thorp and R. H. Crabtree, *Acc. Chem. Res.*, 1991, **24**, 311; L. Que and A. E. True, *Prog. Inorg. Chem.*, 1990, **38**, 97; C. Philouze, G. Blondin, S. Ménage, N. Auger, J.-J. Girerd, D. Vigner, M. Lance and M. Nierlich, *Angew. Chem., Int. Ed. Engl.*, 1992, **31**, 1629; C. Philouze, G. Blondin, J.-J. Girerd, J. Guilhem, C. Pascard and D. Lexa, *J. Am. Chem. Soc.*, 1994, **116**, 8557; V. J. DeRose, I. Mukerji, M. J. Latimer, V. K. Yachandra, K. Sauer and M. P. Klein, *J. Am. Chem. Soc.*, 1994, **116**, 5239.
- P. D. W. Boyd, Q. Li, J. B. Vincent, K. Folting, H.-R. Chang, W. E. Streib, J. C. Huffman, G. Christou and D. N. Hendrickson, *J. Am. Chem. Soc.*, 1988, **110**, 8537; D. P. Goldberg, A. Caneschi and S. J. Lippard, *J. Am. Chem. Soc.*, 1993, **115**, 9299; H.-L. Tsai, H. J. Eppley, N. de Vries, K. Folting, G. Christou and D. N. Hendrickson, *J. Chem. Soc., Chem. Commun.*, 1994, 1745.
- M. W. Wemple, H. L. Tsai, K. Folting, D. N. Hendrickson and G. Christou, *Inorg. Chem.*, 1993, **32**, 2025; C. J. Gomez-Garcia, E. Coronado, P. Gomez-Romero and N. Casan-Pastor, *Inorg. Chem.*, 1993, **32**, 3378; M. Wesolek, D. Meyer, J. A. Osborn, A. De Cian, J. Fischer, A. Derory, P. Legoll and M. Drillon, *Angew. Chem., Int. Ed. Engl.*, 1994, **33**, 1592; R. Cortés, L. Lezama, J. L. Pizarro, M. I. Arriortua, X. Solans and T. Rojo, *Angew. Chem., Int. Ed. Engl.*, 1994, **33**, 2488.
- J. K. McCusker, H. G. Jang, S. Wang, G. Christou and D. N. Hendrickson, *Inorg. Chem.*, 1992, **31**, 1874; S. Wang, H.-L. Tsai, W. E. Streib, G. Christou and D. N. Hendrickson, *J. Chem. Soc., Chem. Commun.*, 1992, 677 and refs. therein; M. W. Wemple, H.-L. Tsai, W. E. Streib, D. N. Hendrickson and G. Christou, *J. Chem. Soc., Chem. Commun.*, 1994, 1031.
- D. A. Bardwell, J. C. Jeffery and M. D. Ward, *Inorg. Chim. Acta*, in the press.

Received 10th May 1995; Paper 5/02966J